Cancer Science
The official journal of the Japanese Cancer Association

13-Cis retinoic acid can enhance the antitumor activity of non-replicating Sendai virus particle against neuroblastoma

Motonari Nomura,[1,2] Takashi Shimbo,[1,5] Yasuhide Miyamoto,[3] Masahiro Fukuzawa[2] and Yasufumi Kaneda[1,4]

[1]Division of Gene Therapy Science, Osaka University, [2]Department of Pediatric Surgery, Graduate School of Medicine, Osaka University, [3]Department of Immunology, Osaka Medical Center for Cancer and Cardiovascular Diseases, Osaka, Japan

(Received August 21, 2012/Revised October 23, 2012/Accepted November 1, 2012/Accepted manuscript online November 7, 2012/Article first published online December 07, 2012)

Hemagglutinating virus of Japan-envelope (HVJ-E) is a drug delivery vector based on inactivated Sendai virus. Recently, antitumor activities were found for HVJ-E itself and clinical trials of HVJ-E for some malignant tumors are now ongoing. We investigated the *in vitro* and *in vivo* antitumor effects of HVJ-E against neuroblastoma, which is one of the most common malignant solid tumors in childhood. The sensitivity of human neuroblastoma cell lines to HVJ-E correlated with the expression level of gangliosides, Sialylparagloboside (SPG) and GD1a, receptors for HVJ. Among the cell lines, SK-N-SH was the most sensitive to HVJ-E *in vitro* and total SPG and GD1a expression was the highest. Complete eradication of subcutaneous tumors derived from SK-N-SH cells was achieved by intratumoral injection of HVJ-E in SCID mice and no recurrence was observed for more than 300 days after HVJ-E inoculation. In contrast, NB1 cells expressed the lowest amount of GD1a and SPG and were resistant to HVJ-E *in vitro*. The expression of GD1a increased by 13-cis retinoic acid (13cRA), which is a therapeutic drug for high risk neuroblastoma, thus leading to an improved sensitivity to HVJ-E *in vitro*. Only growth inhibition of the subcutaneous tumors derived from NB1 cells was achieved by HVJ-E in the SCID mice, but the combination of 13cRA and HVJ-E could achieve partial eradication of the xenograft and also lead to an improved prognosis. In conclusion, HVJ-E is a promising therapeutic modality for neuroblastoma and 13cRA can be used as an adjuvant to HVJ-E. (*Cancer Sci* 2013; 104: 238–244)

Neuroblastoma is one of the most common malignant solid tumors in children and it is responsible for 12% of deaths associated with cancers in children.(1) Although the overall survival of neuroblastoma patients has improved using aggressive therapies in the past decades,(2,3) nearly 50% of high-risk neuroblastoma patients present with widespread dissemination of tumors and the long-term outcome is still very poor, even if intensive multimodal therapies are performed.(4) Some of these treatments are mutagenic, for example, radiotherapy causes somatic mutations in humans and germline mutations in animals.(5) Therefore, an alternative and less toxic cancer therapy is needed, especially for children.

It was reported that cancer cells could be killed after virus infection(6) and various viruses have therefore been used for cancer therapy.(6,7) Recently, we reported that UV-treated non-replicating Sendai virus (also known as hemagglutinating virus of Japan; HVJ) particle named HVJ-envelope (HVJ-E) can induce apoptosis in castration-resistant human prostate cancer cells and human glioblastoma cells (8–10) without toxicity in normal cells. Intratumoral injection of HVJ-E completely eradicated tumor masses of prostate cancer cells and glioblastoma cells in immunodeficient mice.(8,9) Furthermore, we discovered that HVJ-E also stimulated an antitumor immune response by activating cytotoxic T lymphocytes and natural killer (NK) cells and suppressing regulatory T cells.(11,12) Based on these direct and indirect antitumor activities, clinical trials to treat melanoma patients and castration-resistant prostate cancer patients with HVJ-E are now ongoing in Japan.

The mechanism underlying the direct antitumor activity of HVJ-E in neuroblastoma cells is being investigated to confirm whether a similar signaling pathway is involved in neuroblastoma cells, as has been suggested in prostate cancer and glioblastoma cells. Apart from the mechanism, the binding of HVJ-E to its receptor gangliosides is required for inducing cancer cell death. In the present study, we quantified the level of receptors for HVJ in various neuroblastoma cell lines and attempted to increase the expression of these receptors.

Among the recent therapies for advanced neuroblastoma patients, 13-cis retinoic acid (13cRA) is used for maintenance after high-dose chemotherapy combined with bone marrow transplantation.(2,3) It is well known that 13cRA can induce the differentiation of cancer cells from an immature form to a mature form,(13,14) but it is also known that 13cRA can alter the expression pattern of gangliosides.(15) Among the gangliosides, we focused on the possible changes in the synthesis of sialylparagloboside (SPG) and GD1a, receptors for HVJ,(16) because the expression of SPG or GD1a might be necessary for the interaction of HVJ with the target cells.

We concluded that many neuroblastoma cells were sensitive to HVJ-E, and this sensitivity correlated with the expression level of the HVJ receptor gangliosides. Furthermore, 13cRA enhanced the expression of HVJ receptors.

Materials and Methods

Cell lines and mice. Human neuroblastoma cell lines were obtained from the Health Science Research Resources Bank (Tokyo, Japan), European Collection of Animal Cell Cultures (Porton Down, UK) and the RIKEN Cell Bank (Ibaragi, Japan). The primary skin fibroblast cell NSF1227 derived from the forearm skin of a healthy man was established in our laboratory. NB1, NB19 and NB69 cells were maintained in RPMI-1640 (Nacalai Tesque Inc., Kyoto, Japan) supplemented with 15% fetal bovine serum (FBS), 100 IU/mL penicillin and 100 μg/mL streptomycin. SK-N-SH, SK-N-AS, SK-N-BE(2), IMR-32 and NSF1227 cells were maintained in Dulbecco's modified Eagle's medium (Nacalai Tesque Inc.) supplemented with 10% FBS, 100 IU/mL penicillin and 100 μg/mL streptomycin. Cells were incubated at 37°C in a humidified atmosphere of 95% air and 5% CO_2. Five-week-old female C.B-17

[4]To whom correspondence should be addressed.
E-mail: kaneday@gts.med.osaka-u.ac.jp
[5]Present address: Laboratory of Molecular Carcinogenesis, National Institute of Environmental Health Sciences, Research Triangle Park, North Carolina, USA.

doi: 10.1111/cas.12063

/lcr-scid/scidJcl mice were purchased from CLEA Japan Inc. (Tokyo, Japan) and maintained in a temperature-controlled, pathogen-free room. All animals were handled according to the approved protocols and guidelines of the Animal Committee of Osaka University.

Preparation of HVJ-E. HVJ (VR-105 parainfluenza1 Sendai/52, Z strain from American Type Culture Collection) was amplified in chorioallantoic fluid of 10–14-day-old chicken eggs and purified by centrifugation and inactivated by UV irradiation (99 mJ/cm^2), as described previously.[17] The inactivated virus lost the ability of viral genome replication and viral protein synthesis, but retained activity for membrane fusion.[17]

Cell proliferation assay. A MTS assay using CellTiter 96 AQueous One Solution Cell Proliferation Assay Kit (Promega, Tokyo, Japan) was applied to evaluate cell viability. Cells were seeded in 24-well plates (5×10^4 cells/well in 500 μL of medium). Twenty-four hours later the cells were treated with HVJ-E (multiplicity of infection [MOI]: 100–10 000). Forty-eight hours after the treatment with HVJ-E, 100 μL of CellTiter 96 Aqueous One Solution Reagent was added to each well and the plates were incubated at 37°C. After transferring 100 μL of incubation medium from each well into a new 96-well plate, the absorbance at 490 nm was measured.

Pretreatment with 13-cis retinoic acid. Before HVJ-E treatment, NB1 or NSF1227 cells were treated with 10 μM 13-cis retinoic acid (Sigma, St Louis, MO, USA) for 24 h.

Interaction of PKH26-labeled HVJ-E with cells. The HVJ-E (3×10^{10} particles) was suspended in 1 mL Diluent C buffer and incubated with 1 mL of 4 mM PKH26 in Diluent C buffer at room temperature for 5 min (PKH26 Red Fluorescent Cell Linker Kit; Sigma). Labeling was stopped with 2 mL FBS. The labeled HVJ-E was washed with PBS and resuspended in 3 mL PBS. The day before HVJ-E treatment, cells were plated onto cover glasses in six-well plates (3×10^5 cells/well). The cells were incubated with PKH26-labeled HVJ-E (MOI of 10) at 37°C for 4 h, washed with PBS and fixed with 4% paraformaldehyde. Finally, the cells were stained with DAPI and observed using a confocal microscope.

Analysis of acidic glycosphingolipids from neuroblastoma cells. The majority of the experimental procedures have been reported previously.[8,18] Briefly, the acidic glycosphingolipids were extracted from each neuroblastoma cell line and the NSF1227 cell line (1×10^6 cells) and digested with recombinant endoglycoceramidase II from *Rhodococcus* sp. (Takara Bio, Shiga, Japan). The released oligosaccharides were labeled with 2-aminopyridine and separated using a high-performance liquid chromatography (HPLC) system equipped with a fluorescence detector. Normal-phase HPLC was performed on a TSK gel Amide-80 column (Tosoh, Tokyo, Japan). The molecular size of each PA-oligosaccharide is given in glucose units (Gu) based on the elution times of PA-isomaltooligosaccharides. Reversed-phase HPLC was performed on a TSK gel ODS-80Ts column (Tosoh). The retention time of each PA-oligosaccharide is given in glucose units based on the elution times of PA-isomaltooligosaccharides. Thus, a given compound on these two columns provides a unique set of Gu (amide) and Gu (ODS) values, which correspond to coordinates of the 2-D map. PA-oligosaccharides were analyzed using LC/ESI MS/MS. Standard PA-oligosaccharides, PA-GM1 and PA-GD1a, were purchased from Takara Bio and PA-LST-a and PA-SPG were obtained from our previous study.[19]

Real-time quantitative RT-PCR. RNA was extracted from cultured cells using the RNeasy Mini Kit (Qiagen Japan, Tokyo, Japan) and 1 μg total RNA was converted to cDNA with a High-Capacity cDNA Reverse Transcription Kit (Applied Biosystems, Tokyo, Japan). Human ST3GAL1, ST3GAL2, ST3GAL6 and β-actin were amplified using SYBR Premix Ex Taq (Takara Bio). All procedures were performed according to the manufacturer's instructions. The primers were as follows: human ST3GAL1-fp, 5′-GACTTGGAGTGGGTGGTGAG-3′; human ST3GAL1-rp, 5′-GGAACCGGGATGTAGGTGT-3′; human ST3GAL2-fp, 5′-GTCCAGAGGTGGTGGATGAT-3′; human ST3GAL2-rp, 5′-CAGCACCTCATTGGTGTTGT-3′; human ST3GAL6-fp, 5′-AGCCTGGTCCCTCTTTCG-3′; human ST3GAL6-rp, 5′-GGCCACAAGATACCCTCTCA-3′; human β-actin-fp, 5′-GAGCTACGAGCTGCCTGACG-3′; and human β-actin-rp, 5′-GTAGTTTCGTGGATGCCACAG-3′.

Tumor growth *in vivo*. Viable SK-N-SH cells (1×10^7 cells) were resuspended in 100 μL PBS and injected into the subcutaneous space on the back of SCID mice (day 0). When each tumor had grown to 90–110 mm^3, the mice were treated with intratumoral injections of HVJ-E (5000 HAU = 1.5×10^{10} particles in 100 μL PBS) or 100 μL PBS on days 6, 9 and 12. Tumor volume was measured in a blinded manner with slide calipers using the following formula: tumor volume (mm^3) = length × (width)^2/2.

Viable NB1 cells (1×10^7 cells) were resuspended in 100 μL PBS with or without 300 ng 13cRA and injected into the subcutaneous space on the back of the SCID mice. When each tumor had grown to 90–110 mm^3, the mice were treated with intratumoral injections of either HVJ-E (5000 HAU) or 100 μL PBS on days 6, 9, 12 and 15. A second intratumoral injection of 100 μL PBS with or without 300 ng 13cRA was performed on day 18 and HVJ-E treatment was performed again on days 21, 24, 27 and 30. Tumor volume was measured the same way as the SK-N-SH model.

Statistical analyses. Data are expressed as mean ± standard deviation. The two-tailed unpaired Student's *t*-test was used to determine the statistical significance of any differences between two groups. Probability values of $P < 0.05$ were considered to be statistically significant.

Results

Antitumor activity of HVJ-E against human neuroblastoma cell lines *in vitro*. A MTS assay was performed to evaluate cell viability and showed that the survival rates of SK-N-SH, SK-N-AS, SK-N-BE(2), NB19 and NB69 cells decreased by HVJ-E treatment in a dose-dependent manner, and SK-N-SH was the most sensitive to HVJ-E. In contrast, NB1 and IMR32 were not sensitive (Fig. 1a). As it has been reported that the malignancy of neuroblastoma correlates with MYCN amplification, we analyzed the expression of MYCN in each neuroblastoma cell line. A high level of MYCN expression was detected in SK-N-BE(2), IMR32, NB1 and NB19, but not in SK-N-SH, SK-N-AS and NB69 (Data S1, S2, Fig. S1). These results suggest that the sensitivity of neuroblastoma cells to HVJ-E is independent of MYCN. Using PKH26-labeled HVJ-E, SK-N-SH was found to have a stronger affinity for HVJ-E than NB1 and IMR32 (Fig. 1b), implying that the decreased survival of neuroblastoma cells might correlate with their affinity for HVJ-E.

Correlation of antitumor activity of HVJ-E with the expression of SPG or GD1a. To identify the limiting factor related to the sensitivity of cells to HVJ-E, we analyzed the expression levels of receptors for HVJ in each neuroblastoma cell line. It is known that gangliosides with sialylated terminal galactose residue can be receptors for HVJ. Among them, GD1a and SPG are thought to be representative receptors for HVJ. The expression pattern of acidic gangliosides in each cell line was analyzed using HPLC and each peak indicated the expression level of the corresponding ganglioside (Fig. 2a). The rate of each ganglioside's expression could therefore be estimated by calculating the area of each peak (Fig. 2b). An inverse correlation of

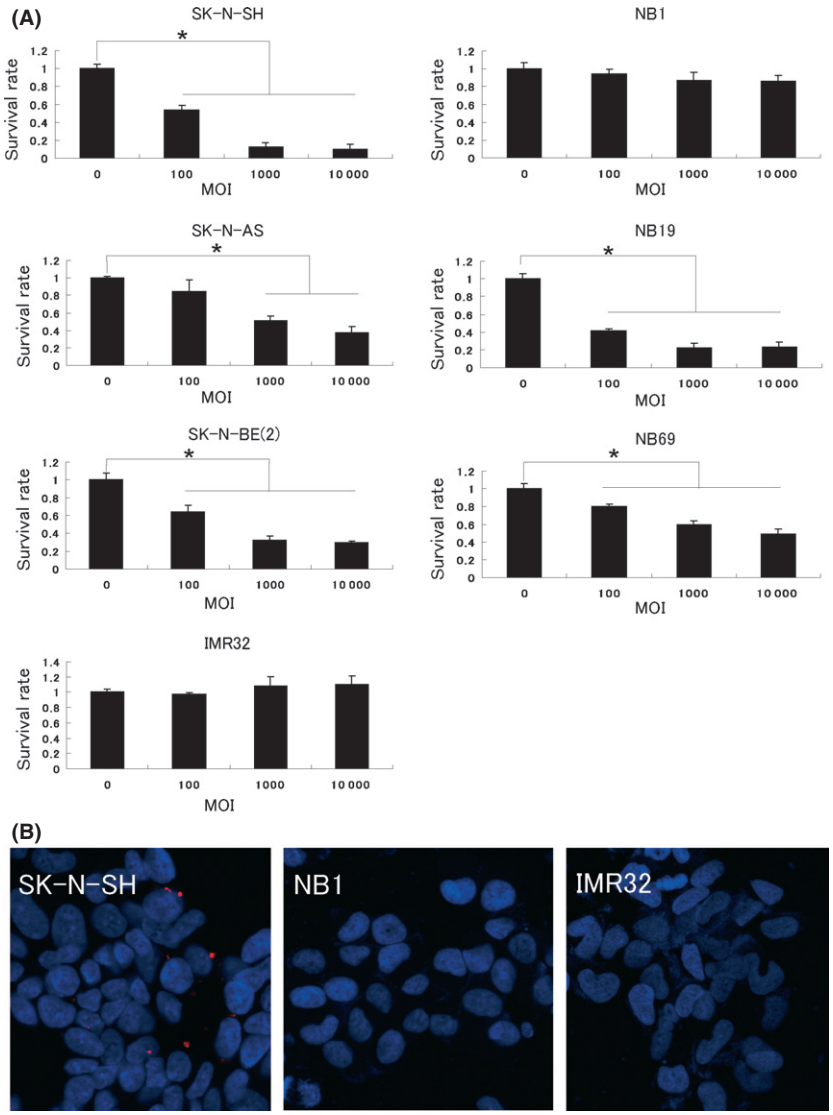

Fig. 1. Antitumor activity of hemagglutinating virus of Japan-envelope (HVJ-E) against neuroblastoma cell lines *in vitro*. (a) Each cell line was treated with a different multiplicity of infection (MOI) of HVJ-E for 48 h and then the survival rate was assessed using a MTS assay. Each value (mean ± standard deviation, $n = 4$) of survival was the ratio to the value without treatment. (b) The interaction of HVJ-E with the neuroblastoma cell lines SK-N-SH, NB1 and IMR32 was assessed. Each cell line was treated with 10 MOI of PKH26 (red)-labeled HVJ-E for 4 h. Nuclei were stained with DAPI (blue). Experiments were repeated three times and representative results are shown. $*P < 0.05$.

the cell survival rate with the expression rate of SPG, GD1a or SPG and GD1a was found (Fig. 2c).

Antitumor activity of HVJ-E against xenograft tumors derived from SK-N-SH cells. We first chose the SK-N-SH cell line, the most sensitive to HVJ-E, to show the antitumor effects of HVJ-E *in vivo*. Tumor volume significantly decreased by three intratumoral injections of HVJ-E (Fig. 3a) and all of the xenografted tumors were completely eradicated by HVJ-E treatment by day 49 after tumor inoculation (Fig. 3b). We also followed the prognosis of mice to prove the safety of HVJ-E. All mice in the PBS-treated group died within 100 days after tumor inoculation, but all mice in the HVJ-E-treated group survived more than 300 days without tumor recurrence or signs of toxicity (Fig. 3c). Thus, the first objective of the present study to show the antitumor effects of HVJ-E against human neuroblastoma *in vitro* and *in vivo* was successfully achieved.

Enhancement of antitumor activity of HVJ-E against the NB1 cell line by 13cRA *in vitro*. The next concern was how to kill the neuroblastoma cell lines that have a very low level of HVJ receptors. Since Hettmer *et al.*[15] reported that retinoic acid could alter the synthesis of the gangliosides of neuroblastoma cell lines, we hypothesized that the synthesis of GD1a might be altered by 13cRA. We chose the NB1 cell line as a model for this experiment, because the expression of SPG and GD1a was the lowest in this cell line out of the numerous cell lines used in the present study. Twenty-four hours after the treatment with 13cRA, the expression pattern of gangliosides was analyzed using HPLC. Each peak of the gangliosides was changed (Fig. 4a). The expression rate of GD1a increased by 13cRA, but the expression of SPG remained unchanged (Fig. 4b). Dimethylsulfoxide, which was used as the solvent for 13cRA, did not affect the synthesis of GD1a (data not shown).

To explain this facilitation of GD1a synthesis, we quantified the expression of sialyltransferases ST3GAL1 and ST3GAL2, which convert GM1 to GD1a,[20] using real-time PCR. The expression of ST3GAL2 was significantly enhanced by 13cRA (Fig. 4c). ST3GAL6, which synthesizes SPG,[20] was not detectable (data not shown). Next, we assessed the 13cRA-induced changes in the sensitivity to HVJ-E by MTS assay. The survival rate of NB1 cells significantly decreased using HVJ-E in the 13cRA-pretreatment group (Fig. 4d). The interaction of HVJ-E with NB1 cells was also strengthened by 13cRA, which was confirmed using PKH26-labeled HVJ-E (Fig. 4e). These data imply that 13cRA can enhance the antitumor activity of HVJ-E by altering the synthesis of ganglioside GD1a in NB1 cells. To ensure the safety of HVJ-E or 13cRA for normal cells, we also analyzed the expression of the gangliosides in the primary skin fibroblast cell line NSF1227.

doi: 10.1111/cas.12063

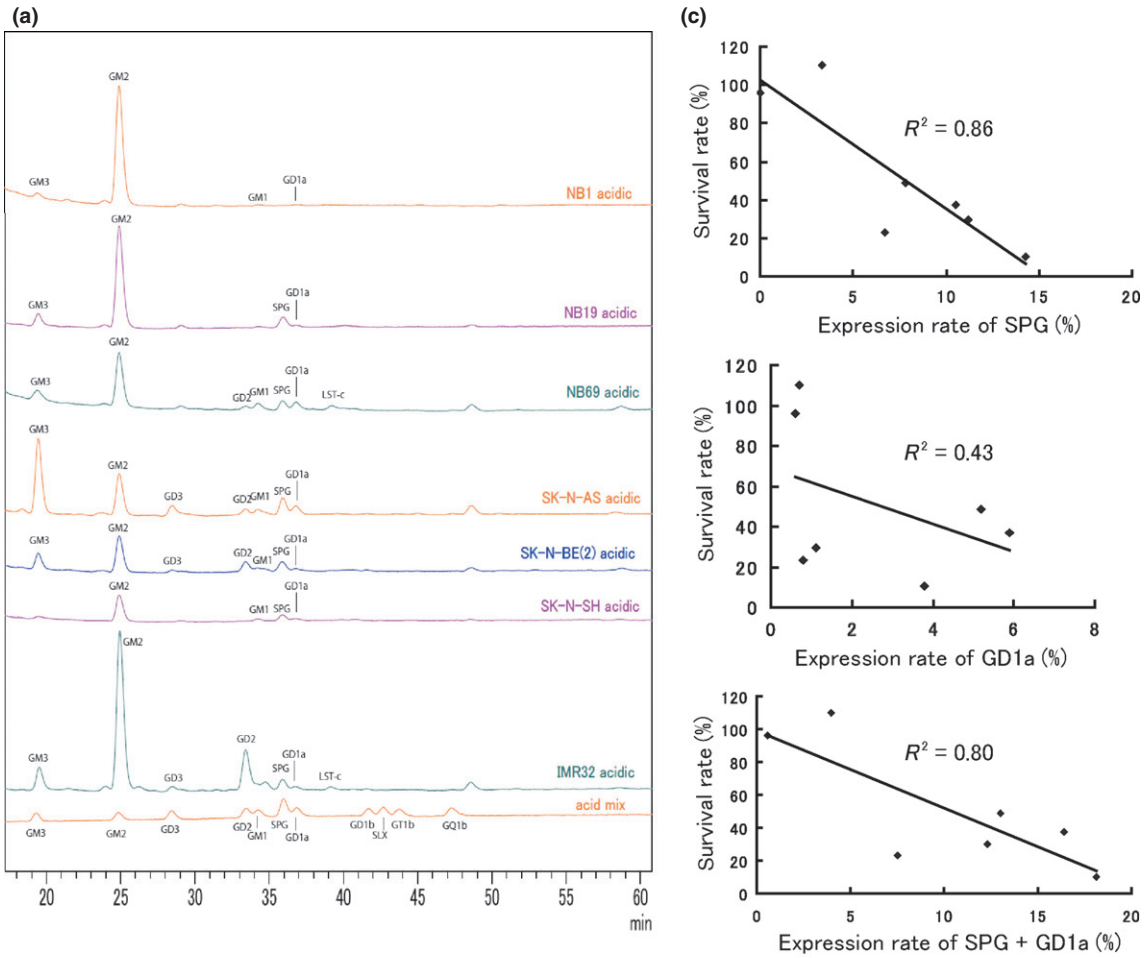

(b)

Rate of expression (%)

	GM3	GM2	GD3	GD2	GM1	SPG	GD1a	LST-c	total
NB1	2.5	94.9	1.3	–	0.8	–	0.6	–	100
NB19	7.2	83.9	1.5	–	–	6.7	0.8	–	100
NB69	10.3	65.2	2.3	2.2	3.9	7.8	5.2	3.0	100
SK-N-AS	44.7	28.9	4.7	3.5	3.8	10.5	5.9	–	100
SK-N-BE(2)	19.4	52.5	1.8	11.2	2.8	11.2	1.1	–	100
SK-N-SH	–	76.9	–	–	5.0	14.3	3.8	–	100
IMR32	8.7	69.5	1.1	15.5	–	3.3	0.7	1.1	100

Fig. 2. Relationship between the expression pattern of gangliosides and hemagglutinating virus of Japan-envelope (HVJ-E)-induced cell death. (a) Cells (1×10^6) of each cell line were collected and then the expression pattern of gangliosides was analyzed using HPLC; (b) the expression rate of each ganglioside was then calculated. (c) The XY scatter plots showed an inverse correlation between the cell survival rate and the expression of SPG or GD1a. R^2 is the Pearson's correlation coefficient index. $R^2 > 0.4$ indicates a relatively strong correlation.

SPG and GD1a were expressed in NSF1227, but the expression pattern was not changed with the 13cRA treatment (Fig. S2A,B). Moreover, NSF1227 cells were not killed by either HVJ-E alone or the combination of 13cRA and HVJ-E (Fig. S2C).

Enhancement of antitumor activity of HVJ-E against xenograft tumors derived from NB1 cells by 13cRA. Based on the findings from the *in vitro* experiments, we tested the antitumor effect of HVJ-E in the NB1-derived tumors xenografted into SCID mice. One treatment protocol comprising five injections was repeated twice. The first injection included 13cRA or PBS. For the other injections, either HVJ-E or PBS was used. More association of PKH26-labeled HVJ-E with cancer cells in the tumor mass was observed in mice treated with 13cRA compared with PBS (Data S3, Fig. S3A). The tumor volume of the 13cRA-treated groups (13cRA + PBS, 13cRA + HVJ-E) was significantly smaller in comparison with the 13cRA-untreated groups (PBS, HVJ-E). Moreover, the combination of 13cRA and HVJ-E almost completely eradicated the NB1-derived tumors. We also confirmed that the combination of 13cRA and HVJ-E induced both apoptosis and necrosis in the xenograft, although HVJ-E alone induced only apoptosis in the edge of the xenograft (Data S4, Fig. S3B).

Although these results were different from the findings obtained from *in vitro* experiments, the tumor volume of the HVJ-E group was significantly smaller than that of the PBS group (Fig. 5a,b). The expression of MICA/MICB, which is

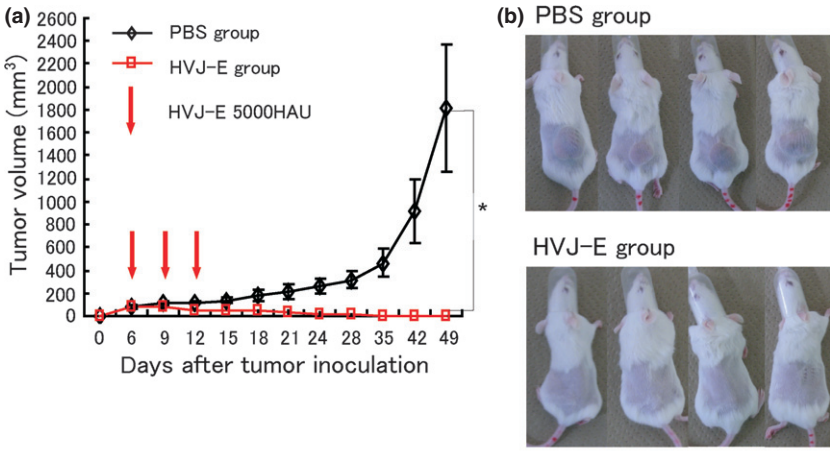

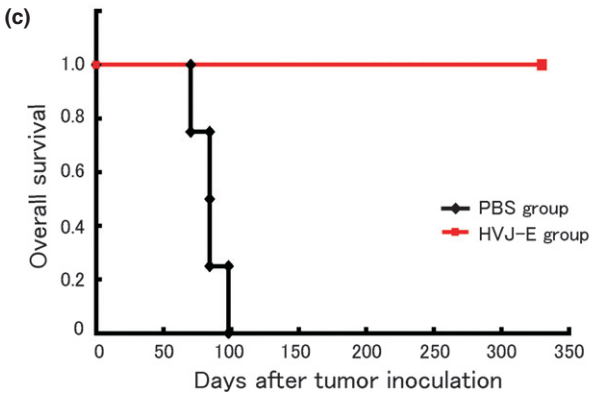

Fig. 3. Antitumor activity of hemagglutinating virus of Japan-envelope (HVJ-E) against xenograft SK-N-SH tumors in SCID mice. (a) Each value (mean ± standard deviation, $n = 4$) of the tumor volume was compared between the PBS and HVJ-E groups. (b) Complete eradication of tumors was achieved in the HVJ-E group by day 49 after tumor inoculation. (c) The overall survival was evaluated using Poisson's regression curve. No recurrence was observed in the HVJ-E group. *$P < 0.05$.

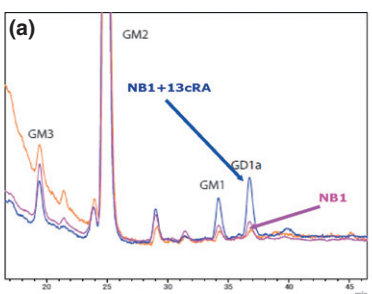

(b)

	Rate of expression (%)								
	GM3	GM2	GD3	GD2	GM1	SPG	GD1a	LST-c	total
NB1	2.5	94.9	1.3	–	0.8	–	0.6	–	100
NB1+13cRA	2.9	87.0	2.1	–	3.0	–	5.0	–	100

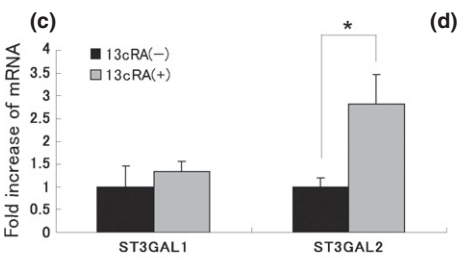

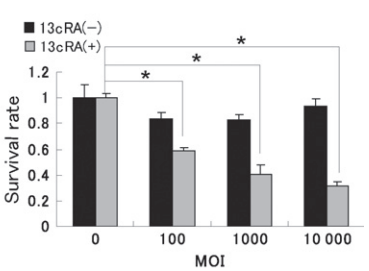

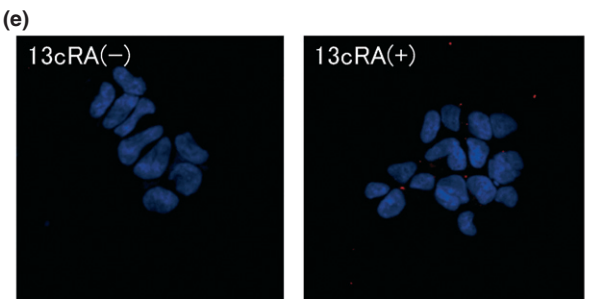

Fig. 4. Effects of 13cRA on the expression of gangliosides in NB1 cells and sensitivity to hemagglutinating virus of Japan-envelope (HVJ-E) *in vitro*. (a) NB1 cells with or without pretreatment using 10 μM 13cRA were collected and the expression pattern of gangliosides was analyzed using HPLC. (b) The expression rate of each ganglioside was calculated. Pretreatment with 13cRA enhanced the expression rate of GD1a. (c) The mRNA expression of ST3GAL1 and ST3GAL2 was analyzed using real-time PCR. Pretretament with 13cRA enhanced the mRNA expression of ST3GAL2. Each value (mean ± standard deviation, $n = 3$) of mRNA was the ratio to the value without treatment. (d) NB1 cells with or without 13cRA pretreatment were exposed to different multiplicity of infection (MOI) of HVJ-E for 48 h and the cell survival rate was then assessed using a MTS assay. Each value (mean ± standard deviation, $n = 4$) of survival was the ratio to the value without HVJ-E treatment. (e) The interaction of HVJ-E with NB1 cells with or without 13cRA pretreatment was assessed. NB1 cells were treated with 10 MOI of PKH26 (red)-labeled HVJ-E for 4 h. Nuclei were stained with DAPI (blue). Experiments were repeated three times and representative results are shown. *$P < 0.05$.

doi: 10.1111/cas.12063

the ligand for NKG2D on NK cells, was endogenously expressed in NB1 cells (Data S2, Fig. S4A), suggesting that NK cells in SCID mice can interact with NB1 cells. The mRNA expression of activated NK cell markers, CD69 and Interferon-gamma (IFN-γ), as well as CD49b (NK cell marker) in the xenograft of each group was also analyzed. HVJ-E alone could enhance the expression of CD49b, CD69 and IFN-γ in the xenografts (Data S1, Fig. S4B). It is likely that the activated NK cells infiltrated the tumor tissue and attacked the tumor cells *in vivo* without the direct interaction of HVJ-E and tumor cells. We performed only two cycles of each therapy because the first mouse in the PBS group died on day 33 after tumor inoculation. We also followed the prognosis of each group. The tumors of the HVJ-E-untreated groups (PBS, 13cRA + PBS) immediately re-grew and all mice in these groups soon died. Within a few weeks after the final treatments, the tumors of the mice in the HVJ-E-treated groups (HVJ-E, 13cRA + HVJ-E) also re-grew. The best prognosis of these mice was obtained in the 13cRA + HVJ-E group (Fig. 5c).

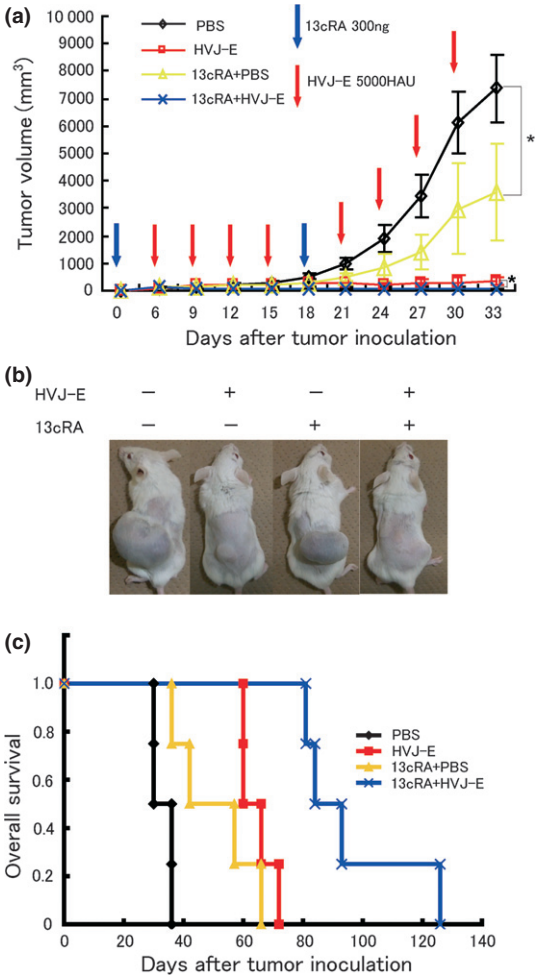

Fig. 5. Antitumor activity of hemagglutinating virus of Japan-envelope (HVJ-E) against xenograft NB1 tumors in SCID mice and the improvement of its activity using 13cRA. (a) Tumor volumes (mean ± standard deviation, $n = 4$) were compared among PBS, HVJ-E, 13cRA + PBS and 13cRA + HVJ-E groups. (b) The representative external appearance of xenografts from each group on day 33 after tumor inoculation showed the superiority of the combination of 13cRA and HVJ-E. (c) Overall survival was evaluated using a Poisson's regression curve. The best prognosis was obtained in the 13cRA + HVJ-E group. *$P < 0.05$.

Therefore, the second objective of the present study, to enhance the sensitivity of a HVJ-E-resistant human neuroblastoma cell line to HVJ-E *in vitro* and *in vivo*, was also successfully achieved.

Discussion

In the past few decades many genetic features of neuroblastoma have been identified that correlate with the clinical outcome. Among them, MYCN amplification is one of the most critical risk factors in neuroblastoma patients and many patients classified into the high-risk group have MYCN amplification with a poor prognosis.[21] Herein, we demonstrated that HVJ-E could kill human neuroblastoma cells, even if MYCN was amplified.

Hemagglutinating virus of Japan is a mouse parainfluenza virus belonging to the paramixoviridae genus. Two glycoproteins, fusion (F) and hemagglutinin-neuraminidase (HN), are present on the viral envelope.[22] The first step of infection involves the binding of HN to its receptors. Hemagglutinin-neuraminidase has a neuraminidase activity and is thought to digest carbohydrate chains on the viral envelope. Following this, the hydrophobic region of the F protein, which is thought to function as a fusion peptide, invades the lipid bilayer through its association with lipid molecules such as cholesterol.[23] Therefore, the first step of infection requires expression of HN receptors SPG and GD1a. The results from the present study imply that the expression levels of SPG and GD1a can be used to predict the response to HVJ-E therapy. Therefore, neuroblastoma cells with a low expression of SPG and GD1a are likely to be resistant to HVJ-E and the increase of these gangliosides is necessary to overcome such resistance.

Therefore, we demonstrated that 13cRA might be a promising agent for the enhancement of the expression of SPG or GD1a. It has been known that 13cRA has the ability to induce cellular differentiation and to decrease the proliferation of neuroblastoma cells *in vitro*.[13] In the steady state, retinoic acid receptor (RAR) makes a heterodimer with retinoid X receptor (RXR) and this RAR–RXR heterodimer binds to retinoic acid response elements (RARE) to repress the acetylation of histones, thereby silencing many genes.[24–26] However, once 13cRA binds to RAR, this repression becomes inhibited and the transcription of silenced genes becomes activated.[27] Therefore, many outcomes other than cellular differentiation can be obtained by the use of 13cRA. Enhancing the expression of ST3GAL2 and the synthesis of GD1a are other examples of 13cRA-induced outcomes.

In the standard protocol for high-risk neuroblastoma, the main therapy consists of surgery, radiotherapy and chemotherapy combined with bone marrow transplantation. The chemotherapy for high-risk patients is very intensive and is sometimes too toxic for children, but it must be administered repeatedly to achieve efficient eradication of tumors. The goal of the final phase of therapy is to eradicate any minimal residual disease (MRD), but these repeated chemotherapies often induce chemoresistance, therefore other agents for chemoresistant MRD are necessary. As a therapeutic modality for MRD, 13cRA is considered to be useful because of its ability to induce cellular differentiation. Considering the additional ability of 13cRA to enhance the antitumor activity of HVJ-E, a reduction in the cycles of chemotherapy and the earlier use of the combination of 13cRA and HVJ-E might be a novel strategy for high-risk neuroblastoma, especially when severe adverse drug reactions are observed during chemotherapy.

Herein, we demonstrated that 13cRA could enhance the antitumor activity of HVJ-E against NB1 cells, which were resistant to HVJ-E *in vitro*, but HVJ-E alone could also inhibit the tumor growth of NB1-derived xenografts to some degree *in vivo*. This is probably because HVJ-E activates NK cells in SCID mice. HVJ-E can activate NK cells without binding to tumor cells. This is because HVJ-E can directly induce the release of CXCL10 and interferon-β from dendritic cells to elicit the infiltration and activation of NK cells.[12] Our data also show that HVJ-E can activate NK cells without binding to NB1 cells. We used SCID rather than non-obese diabetic-SCID mice for the model of HVJ-E therapy, because the direct antitumor activity of HVJ-E *in vivo* has already been reported and we wanted to eradicate "human" neuroblastoma cell lines in a model closer to normal humans with some antitumor immunity.[8]

In conclusion, HVJ-E might therefore be a useful therapeutic modality for human neuroblastoma if SPG or GD1a are expressed in tumor cells and its anticancer effects can be enhanced by 13cRA. Therefore, combination therapy using HVJ-E and 13cRA might be an effective new method for the treatment of neuroblastoma.

Acknowledgments

This study was supported by the Program for Promotion of Fundamental Studies in Health Sciences of the National Institute of Biomedical Innovation (Project ID: 10-03).

Disclosure Statement

The authors declare no conflicts of interest.

References

1 Surveillance, Epidemiology, and End Results (SEER) Program. SEER*Stat mortality database: total U.S. (1969–2006), National Cancer Institute, DCCPS, Surveillance Research Program. [Cited 3 Aug 2012.] Available from URL: www.cdc.gov/nchs
2 Matthay KK, Villablanca JG, Seeger RC *et al.* Treatment of high-risk neuroblastoma with intensive chemotherapy, radiotherapy, autologous bone marrow transplantation, and 13-cis-retinoic acid. *N Engl J Med* 1999; **341**: 1165–73.
3 Matthay KK, Reynolds CP, Seeger RC *et al.* Long-term results for children with high-risk neuroblastoma treated on a randomized trial of myeloablative therapy followed by 13-cis-retinoic acid: a Children's Oncology Group study. *J Clin Oncol* 2009; **27**: 1007–13.
4 Maris JM, Hogarty MD, Bagatell R, Cohn SL. Neuroblastoma. *Lancet* 2007; **369**: 2106–20.
5 Boice JD Jr, Tawn EJ, Winther JF *et al.* Genetic effects of radiotherapy for childhood cancer. *Health Phys* 2003; **85**: 65–80.
6 Kelly E, Russell SJ. History of oncolytic viruses: genesis to genetic engineering. *Mol Ther* 2007; **15**: 651–9.
7 Newman W, Southam CM. Virus treatment in advanced cancer; a pathological study of fifty-seven cases. *Cancer* 1954; **7**: 106–18.
8 Kawaguchi Y, Miyamoto Y, Inoue T, Kaneda Y. Efficient eradication of hormone-resistant human prostate cancers by inactivated Sendai virus particle. *Int J Cancer* 2009; **124**: 2478–87.
9 Tanaka M., Shimbo T, Kikuchi Y, Matsuda M, Kaneda Y. Sterile alpha motif containing domain 9 (SAMD9) is involved in death signaling of malignant glioma treated with inactivated Sendai virus particle (HVJ-E) or type I interferon. *Int J Cancer* 2010; **126**: 1982–91.
10 Kaneda Y. Update on non-viral delivery methods for cancer therapy; possibilities of DDS with anti-cancer activities beyond delivery as a new therapeutic tool. *Expert Opin Drug Deliv* 2010; **9**: 1079–93.
11 Kurooka M, Kaneda Y. Inactivated Sendai virus particles eradicate tumors by inducing immune responses through blocking regulatory T cells. *Cancer Res* 2007; **67**: 227–36.
12 Fujihara A, Kurooka M, Miki T, Kaneda Y. Intratumoral injection of inactivated Sendai virus particles elicits strong antitumor activity by enhancing local CXCL10 expression and systemic NK cell activation. *Cancer Immunol Immunother* 2008; **57**: 73–84.
13 Sidell N. Retinoic acid-induced growth inhibition and morphologic differentiation of human neuroblastoma cells *in vitro*. *J Natl Cancer Inst* 1982; **68**: 589–96.
14 Abemayor E, Chang B, Sidell N. Effects of retinoic acid on the *in vivo* growth of human neuroblastoma cells. *Cancer Lett* 1990; **55**: 1–5.
15 Hettmer S, McCarter R, Ladisch S, Kaucic K. Alterations in neuroblastoma ganglioside synthesis by induction of GD1b synthase by retinoic acid. *Br J Cancer* 2004; **91**: 389–97.
16 Villar E, Barroso IM. Role of sialic acid-containing molecules in paramyxovirus entry into the host cell: a minireview. *Glycoconj J* 2006; **23**: 5–17.
17 Kaneda Y, Nakajima T, Nishikawa T *et al.* Hemagglutinating virus of Japan (HVJ) envelope vector as a versatile gene delivery system. *Mol Ther* 2002; **6**: 219–26.
18 Hatano K, Miyamoto Y, Nonomura N, Kaneda Y. Expression of gangliosides, GD1a and sialyl paragloboside, is regulated by NF-κB-dependent transcriptional control of α2,3-sialyltransferase I, II and VI in human castration-resistant prostate cancer cells. *Int J Cancer* 2011; **129**: 1838–47.
19 Korekane H, Tsuji S, Noura S *et al.* Novel fucogangliosides found in human colon adenocarcinoma tissues by means of glycomic analysis. *Anal Biochem* 2007; **364**: 37–50.
20 Takashima S. Characterization of mouse sialyltransferase genes: their evolution and diversity. *Biosci Biotechnol Biochem* 2008; **72**: 1155–67.
21 Seeger RC, Brodeur GM, Sather H *et al.* Association of multiple copies of the N-myc oncogene with rapid progression of neuroblastomas. *N Engl J Med* 1985; **313**: 1111–6.
22 Okada Y. Sendai virus-induced cell fusion. *Methods Enzymol* 1993; **221**: 18–41.
23 Kaneda Y. Applications of hemagglutinating virus of Japan in therapeutic delivery systems. *Expert Opin Drug Deliv* 2008; **5**: 221–33.
24 Germain P, Iyer J, Zechel C, Gronemeyer H. Co-regulator recruitment and the mechanism of retinoic acid receptor synergy. *Nature* 2002; **415**: 187–92.
25 Glass CK, Rosenfeld MG. The coregulator exchange in transcriptional functions of nuclear receptors. *Genes Dev* 2000; **14**: 121–41.
26 Hu X, Lazar MA. Transcriptional repression by nuclear hormone receptors. *Trends Endocrinol Metab* 2000; **11**: 6–10.
27 Clarke N, Germain P, Altucci L, Gronemeyer H. Retinoids: potential in cancer prevention and therapy. *Expert Rev Mol Med* 2004; **6**: 1–23.

Supporting Information

Additional Supporting Information may be found in the online version of this article:

Fig. S1. MYCN expression in neuroblastoma cell lines.

Fig. S2. Antitumor activity of HVJ-E or 13cRA against a normal cell line.

Fig. S3. Interaction of HVJ-E with NB1 cells and the detection of apoptosis or necrosis *in vivo*.

Fig. S4. Expression of NK cell–ligands in cancer cells and activation of NK cells in tumor tissue with HVJ-E.

Data S1–S4. Including: primers for real-time quantitative RT-PCR; antibodies and western blotting analysis; interaction of PKH26-labeled HVJ-E with NB1-derived xenografts; and detection of HVJ-E-induced apoptosis and necrosis in NB1-derived xenografts.

doi: 10.1111/cas.12063